JP Journal of Heat and Mass Transfer
Volume 3, Number 3, 2009, Pages 167-197
Published Online: November 26, 2009
This paper is available online at http://www.pphmj.com

MILK FOULING IN A PLATE HEAT EXCHANGER USING DYNAMIC AND ARTIFICIAL NEURAL NETWORKS MODELS

YOUCEF MAHDI[1,2,*] **and LOUNÈS OUFER**[1]

[1]Université des Sciences et de la Technologie Houari Boumediene
Faculté de Génie Mécanique et de Génie des Procédés
Laboratoire des Phénomène de Transfert
B. P. 32, El-Alia, Bab-Ezzouar, Alger, Algérie
e-mail: mahdiyoucef@yahoo.fr

[2]Université Dr Yahia Fares de Médéa
Institut des Sciences et de la Technologie
Quartier Ain D'heb Médéa 26001, Algérie

Abstract

In this article, a neural and two-dimensional dynamic fouling model for milk fouling in a plate heat exchanger is proposed. Emphasis is placed on fouling calculation based on the hydrodynamic and thermodynamic performances of the plate heat exchanger. A 12-channel plate heat exchanger with counter-current flows is used to quantify the milk deposition developed inside the channels. The aggregation rate of unfolded protein is found to increase exponentially with increasing wall temperature and is accompanied by a substantial reduction in the heat transfer coefficient. The neuronal model previously adapted predicts mass deposition, the overall heat transfer coefficient and the critical time. At this time, the unit is stopped for cleaning and reducing the impact of

Keywords and phrases: milk, plate heat exchanger, modeling, fouling, pasteurization, neural networks.

*Corresponding author

Received May 29, 2009

fouling on such processes. The method determines when the cleaning operation is necessary once the system is under critical operational conditions.

Nomenclature

$\overline{C}$	Criterion parameter
$\overline{b}$	Defined variable of neuronal network (current)
$\overline{D}$	Diameter, m
$\bar{f}$	Friction factor
$\overline{E}$	Function error
$\overline{m}$	Mass flow, Kg/s
$\overline{P}$	Simulated parameter value
a	Defined variable of neuronal network (desired)
b	Proportionality constant
Bi	Biot number
C	Bulk protein concentration, kg/m^3
C^*	Protein concentration in thermal boundary layer, kg/m^3
C_p	Specific heat, $KJ/kg^\circ C$
D	Diffusion coefficient, m^2/s
d	Particle diameter, m
E	Activation energy, KJ/mol
e	Gap between the plates, m
f	Function
h	Convective heat transfer coefficient, $W/m^2.^\circ C$
H	Height of plate, m
I	Activity product
i	Sum of linear inputs
k_m	Mass transfer coefficient, m/s

K_s	Deposit constant of calcium phosphate, $\mathrm{kg/m^2 \cdot s}$
K_w	Wall reaction rate constant, $\mathrm{m/s}$
L	Plate length, m
L_L	Solubility product
m	Channel number
Mass_p	Mass of deposit, $\mathrm{g/m^2}$
$\mathrm{N_{av}}$	Avogadro constant
Nu	Nusselt number
P	Pressure, Pa
Pr	Prandtl number
Q	Heat transfer, W
R	Gas constant, $\mathrm{KJ/mol \cdot {}^\circ C}$
Re	Reynolds number
S	Area, $\mathrm{m^2}$
Sc	Schmidt number
Sh	Sherwood number
T	Temperature, $^\circ\mathrm{C}$
t	Time, s
U	Overall heat transfer coefficient, $\mathrm{W/m^2 \cdot {}^\circ C}$
u	Velocity component in x-direction, $\mathrm{m/s}$
V	Molecular volume, $\mathrm{m^3}$
w	Width, m
X	Input neuron

Greek Symbols

ξ	Constant
ρ	Density, $\mathrm{kg/m^3}$
δ	Dynamic boundary layer thickness, m
μ	Dynamic viscosity of fluid, $\mathrm{Pa \cdot s}$

η	Kinematic viscosity, m^2/s
ε	Surface roughness
λ	Thermal conductivity, $W/m \cdot {}^\circ C$
ϑ	Threshold
Γ_i	Connection weights. Defined variable
λ_j	Training gain
ΔP	Pressure drop, Pa
δ_T	Thermal boundary layer thickness, m
$\Delta T_{\log}$	Logarithmic-means temperature difference, $^\circ C$

Subscripts

0	Initial
A	Aggregate protein
amb	Ambient
B	Terminal block
c	Hot
Cr	Critical
d	Deposit
D	Unfolded protein
E	Equivalent diameter
e	Fluid inlet
f	Cold
j	Channel number
M	Deposited protein
N	Native protein
P	Plate number
ref	Reference
s	Fluid outlet
w	Wall

1. Introduction

Food products are subject matter to quite elaborated transformations in order to present qualities that are in conventionality with existing food safety system. Therefore, food producers and manufacturers forever attempt to define the optimal and economic conditions for disinfected processing. This is done by taking into account the physical and biochemical modifications of the raw materials along process production. In case, the happening of fouling constitutes one of the major encountered problems in the concerned processes [4]. This is because it generates restrictions in the thermal performance of equipment which increases the price of production but it can also have a considerable effect on the quality of the product as in the case of the dairy industry [24].

Fouling of plate heat exchangers through milk processing is a major problem with a negative impact on operating costs and product quality. It also leads to an increase in pressure drop across the exchanger and to possible deterioration in product quality due to failure of the process fluid to reach the required temperature. An additional serious problem associated with fouling is the cleaning of fouled surfaces by means of costly and time-consuming techniques where environmentally offensive chemicals are employed. Given the economic impact of fouling in milk heat exchangers, it is not surprising that there is a considerable amount of literature available on modeling of the fouling process. There seems to be an agreement that thermal denaturation of whey protein β-lactoglobulin plays a major role in the fouling process, certainly when the temperature is below 90°C. A secondary fouling process can also concern salts.

A number of authors have modeled fouling occurrence in plate heat exchanger systems based on simplified 1D representation of the process hydrodynamics [1, 9, 22]. For milk, another paper presented a mathematical model for complex plate heat exchanger arrangements subjected to fouling by adapting a plug flow model with added axial convection and radial dispersion effects [8]. However, the presented models were based on 1D hydrodynamic performance of the plate heat exchanger, which is a considerable simplification of the effect of plate geometry used in industry. In previous studies such as those by Georgiadis and Macchiatto [8], a 2D model accounting for the hydrodynamics of fluid flow was used to predict the temperature distribution of flow with higher accuracy than a one-dimensional model. The latter model led to larger prediction errors for plate heat exchanger with a larger plate aspect ratio. To our knowledge, the study of such problems by a specific 2D

modeling including mass and energy balances, such as described in the considered paper is nearly non-existent.

Recently, some authors have used artificial intelligence as a substitute method for the fouling prediction. Shetty and Chellam [23] presented papers about the prediction of fouling using artificial neural networks in micro-filtration; Zhang et al. [27] used this technique in the evaluation of fouling in batch polymerization reactor on a laboratory scale. Riverol [20, 21] and Lalot and Lecoeuche [16] formulated work for the fouling detection and evaluation of the overall heat transfer coefficient. Several papers are devoted to the prediction of long-term fouling and they do not offer cleaning schedules that can be implemented on an industrial size. For milk, the creation of fouling needs only few hours; as result, the pasteurization units start to work in critical conditions a few hours after they start up. Artificial neural networks are an adequate instrument to evaluate problems, although they are not always the best. Neural networks are often used as a black box modeling plan where the characterization of adequate inter-relations is necessary. Though, insight into the process can help the designer to find quickly adequate inter-relations for the neural model. The complete artificial neural networks inter-relations has to comprise the order of the system, the existence of possible constraints and how the correlated inputs can influence the selection of the number of inputs used for the network. The approach suggested in this paper is the application of neural networks, in particular, the Adaline network (Adaptive Linear Element), as a mathematical tool.

The first purpose of the present study is to apply the chemical reaction model in a 2D dynamic model to predict the milk deposit patterns on the plate surfaces with more accuracy. This approach is expected to pave the way to organize and optimize the operating conditions for dropping the extra costs involved with fouling. The second aim is to apply the artificial neural networks for an installation of milk pasteurization to predict the deposited mass fouling of the proteins and salts on the surface of the plates heat exchanger that composes the unit pasteurization, in order to estimate the overall heat transfer coefficient, as well as the critical conditions that imposes the necessity to clean.

2. Mechanisms and Mathematical Model

In the present work, a formulation of the fouling problem occurring inside a plate heat exchanger allowing milk pasteurization is proposed. A 2D mathematical model of the process is presented based on a dynamic behaviour of the flowing fluid (milk). The considered model is based on chemical reaction, mass transfer and

various other factors taking place during thermal treatment of milk. The model is coupled with the dynamic models of a plate heat exchanger, hence resulting in a final model that includes a set of partial differential and algebraic equations. The analysis is carried out to allow parameter evaluation through a dynamic problem optimization. At the end, the model is simulated using a chosen software program (Mathematica 5.0) designed to monitor the dynamic temperature profiles of fluid at different locations.

2.1. System description

The considered pasteurization process occurs in a plate heat exchanger recommended for the pasteurization of milk because it offers an important convection coefficient and higher turbulence in comparison with other classes of heat exchangers. The process consists of heating milk to a given temperature during a certain time in order to eliminate the pathological action of any possible bacteria. This is a necessary treatment that milk must undergo before any further use. Milk flowing from a pre-heating tank enters the heat exchanger where it is heated by hot steam in order to reach the pasteurization temperature.

2.2. The mechanism of fouling

A schematic representation of the proposed fouling model is given in Figure 1. When the milk is heated to a temperature greater than $65^{\circ}C$, the β-lactoglobulin protein is unsteady and becomes the precursor for deposit formation according to two possible mechanisms [14, 15]:

1. The β-lactoglobulin natural protein (*N*-protein) experiences a denaturation process (change of structure) and becomes very reactive because of it is SH bond (β-lactoglobulin denatured form or *D* protein).

2. An irreversible polymerisation reaction resulting in insoluble particles as aggregations noted protein *A* (β-lactoglobulin aggregated form).

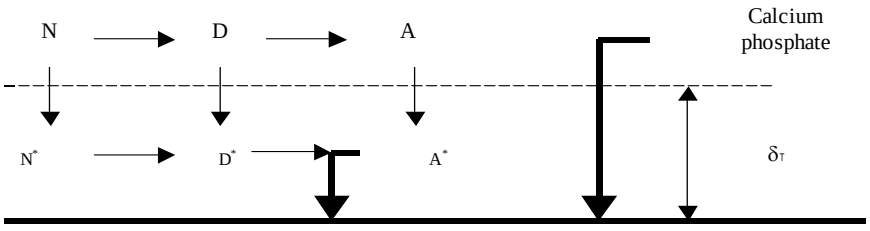

Figure 1. Model of proteins and salts deposition on the heat exchanger surface.

Usually, induction period is extremely short or even instantaneous in plate heat exchangers where intense mixing of fluid held due to high turbulence. Fouling decreases with increasing turbulence [4]. The thickness and subsequently the volume of laminar sublayer decreases with increasing velocity and consequently the amount of foulant depositing on the heat-transfer surface decreases.

2.3. Causes of protein aggregation

The β-lactoglobulin protein has a global structure held together by S-S bonds and one non-exposed internal free SH group. When heated, the β-lactoglobulin starts to unfold. The free thiol group is therefore exposed and the molecule enters into an activated state making it possible to react with another β-lactoglobulin molecule. Therefore, a radical chain may grow to form an aggregate that is able to deposit on the heat transfer surface. It is known that the rate of deposition is related to the concentration of activated molecules in the solution and may be calculated using the model of denaturation and aggregation of the β-lactoglobulin [6, 13].

The kinetics of the different reactions is well known [26]. A mass transfer process of the three forms of the β-lactoglobulin protein takes place between the fluid and the layer limit. The aggregated proteins form the deposit but it is still essential to know the kinetics and the different physical and chemical parameters of the phenomena taking place in order to be able to quantify the extent of this deposit represented by the fouling resistance [13-26].

2.4. Mineral deposition

In addition to the above mentioned type of fouling, the calcium phosphate deposition takes also place and presents an inverse solubility relation with temperature. During the pre-heating process, the ionic product becomes high with relation to the solubility concentration limits. Salts deposit in the form of crystals on the surface of the heat exchanger [12]. Calcium phosphate may also precipitate in the core flow. It may then deposit onto the casein micelle surface and/or onto the β-lactoglobulin molecules contained in the milk serum phase. In all cases, it will in time ultimately form a deposit onto the stainless steel wall of the heat exchanger plates as shown in Figure 1.

Fouling caused by milk constituents is a complex process in which both whey protein aggregation and calcium phosphate formation in the bulk fluid are to be accounted for. The whole fouling mechanism can be described in the following steps:

1. Straight adsorption of a protein mono-layer even at room temperature.

2. Formation of activated β-lactoglobulin molecules in the bulk solution at temperatures higher than 65°C. The β-lactoglobulin aggregates (tenths of nanometers) and calcium phosphate particles are formed.

3. Continuous transport of these foulant particles formed in the bulk to the heated surface. However, some activated molecules can be inactivated during this phase because some given reactions with other molecules in the bulk can make the particles not enough active to create fouling.

4. Deposition of activated molecules by adsorption on the heat exchanger surface. Calcium ions entrapped in the protein deposit may help to stabilize these structures.

5. At relatively high temperatures (above 85°C), the main deposit component is calcium phosphate which offers an open network structure where small protein aggregates can be entrapped.

2.5. Neuronal system description

This work presents a formulation of the fouling problem in plate heat exchanger during milk pasteurization proposed by neuronal networks in order to minimize it, without destabilizing the system and to establish a law of order. For that, we need a precise and simple model to predict all evolution of the variables.

In a first time, the optimal conditions of working are presented to represent desired reference to adapt the chosen neuronal model. Thereafter, it is necessary to consider a minimal surface exchange that permits an optimal working of the heat exchanger. Cleaning becomes necessary when the surface of the heat exchanger becomes inferior to the surface of the minimal exchange recommended. The fouling profiles references are estimated as using previous simulations based on a chemical modeling evolution against similar operative conditions.

The heat exchanger surface is calculated by

$$S = \frac{Q}{U\Delta T_{\log}}, \tag{1}$$

where

$$\Delta T_{\log} = \frac{\Delta T_1 - \Delta T_2}{\log \frac{\Delta T_1}{\Delta T_2}} \tag{2}$$

and

$$\Delta T_1 = T_c^e - T_f^s, \quad \Delta T_2 = T_c^s - T_f^e. \tag{3}$$

Heat thermal flux is calculated by

$$Q = \overline{m_c}(T_c^e - T_c^s) = \overline{m}_f (T_f^s - T_f^e). \tag{4}$$

During the milk pasteurization, fouling of the surface exchange generates a reduction of the flow passage section and reduces the thermal exchanges between the two fluids circulating in the plate heat exchanger because the deposit due to the fouling forms an insulating layer. Once the value of the critical mass deposition Mass_p^{Cr} is reached, the neuronal network operates to recommend cleaning:

$$\text{Mass}_p < \text{Mass}_p^{Cr}. \tag{5}$$

The critical mass of deposit is calculated while considering 15% of global exchange coefficient reduction which leads to a bad pasteurization following an important accumulation of the deposit and require a cleaning of heat exchanger.

3. Mathematical Model of Fouling

3.1. Flow and energy equations

The heat exchanger is supplied with hot water with one channel per pass for a total of five passes. Milk supply is to five channels per pass for a total of five passes. The heat exchanger consists of 12 plates. Assuming that the plate surface is flat and smooth (Figure 2), the governing 2D flow equations include the continuity and the momentum equations in the Cartesian coordinates, as given by the following equations:

$$\frac{\partial u}{\partial x} + \frac{\partial v}{\partial y} = 0, \tag{6}$$

$$\frac{\partial u}{\partial t} + u\frac{\partial u}{\partial x} + v\frac{\partial u}{\partial y} = -\frac{1}{\rho}\frac{\partial P}{\partial x} + \eta\left(\frac{\partial^2 u}{\partial x^2} + \frac{\partial^2 u}{\partial y^2}\right), \tag{7}$$

$$\frac{\partial v}{\partial t} + u\frac{\partial v}{\partial x} + v\frac{\partial v}{\partial y} = -\frac{1}{\rho}\frac{\partial P}{\partial y} + \eta\left(\frac{\partial^2 v}{\partial x^2} + \frac{\partial^2 v}{\partial y^2}\right), \tag{8}$$

where η is the kinematic viscosity, ρ is the density, P is the pressure, t is the time,

and u and v are the velocity components along the x and y directions, respectively. The transient energy equation for a 2D constant property, incompressible flow can be given by

$$e_j \rho_j Cp_j [(\partial T_j / \partial t) + u_j (\partial T_j / \partial x) + v_j (\partial T_j / \partial y)] = U_j (T_{p(j-1)} + T_{pj} - 2T_j), \quad (9)$$

$$Cp_p \rho_p \delta_p \frac{\partial T_{pj}}{\partial t} = U_j (T_j + T_{j+1} - 2T_{pj}), \quad (10)$$

where T_j is the temperature of the fluid in channel j, T_{pj} is the temperature of plate j, Cp_j and Cp_p are, respectively, the specific heats of fluid in channel j and plate p, ρ_j and ρ_p are the respective densities of fluid in channel j and plate p, e_j is the distance between the plates, δ_p is the plate thickness, and U_j is the overall heat transfer coefficient in channel j.

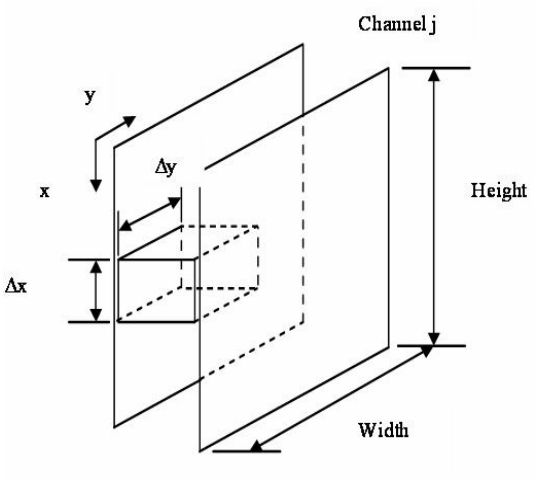

Figure 2. Control volume of fluid inside the channel in 2D.

3.2. Mathematical model

The rate constant expression for the different reactions involved in the protein transformations is of the Arrhenius-type form given by

$$K = K_0 \exp\left[-\frac{E}{RT}\right], \quad (11)$$

where values of K_0 and E are given in Table 1 for different temperatures.

Table 1. Kinetic parameters for the fouling reaction scheme [3]

	$T(^{\circ}C)$	$E(\mathrm{J/mol})$	$\ln(\mathrm{K}_0)$
Native	70-90	2.614×10^{5}	86.41
Denatured	70-90	3.37×10^{37}	89.40
Aggregation	70-90	2.885×10^{5}	91.32

Proteins react in both the fluid bulk and the thermal boundary layer in fluid milk. Native protein N is transformed to denatured protein D, in a first order reaction. The denatured protein then reacts to give aggregated protein A in a second order reaction. Mass transfer between the fluid bulk and the thermal boundary layer takes place for each protein. Only the aggregated protein is deposited on the wall (M). The rate of deposition is proportional to the concentration of aggregated protein in the thermal boundary layer. The fouling resistance to heat transfer is proportional to the thickness of the deposit.

The mass balances in bulk fluid are as follows:

$$\frac{\partial C_{NJ}}{\partial t}+u\frac{\partial C_{NJ}}{\partial x}+v\frac{\partial C_{NJ}}{\partial y}=-K_{N0}\exp\left[-\frac{E_N}{RT_j}\right]C_{NJ}+\frac{\partial}{\partial x}\left[D_N\left(\frac{\partial C_{NJ}}{\partial x}\right)\right]+\frac{\partial}{\partial y}\left[D_N\left(\frac{\partial C_{NJ}}{\partial y}\right)\right]-\frac{k_{mN}}{\delta_T}(C_{NJ}-C^{*}_{Np}). \quad (12)$$

For the denatured protein

$$\frac{\partial C_{DJ}}{\partial t}+u\frac{\partial C_{DJ}}{\partial x}+v\frac{\partial C_{DJ}}{\partial y}=K_{N0}\exp\left[-\frac{E_N}{RT_j}\right]C_{NJ}-k_{D0}\exp\left[-\frac{E_D}{RT_j}\right]C^{2}_{DJ}+\frac{\partial}{\partial x}\left[D_D\left(\frac{\partial C_{DJ}}{\partial x}\right)\right]+\frac{\partial}{\partial y}\left[D_D\left(\frac{\partial C_{DJ}}{\partial y}\right)\right]-\frac{k_{mD}}{\delta_T}(C_{DJ}-C^{*}_{Dp}). \quad (13)$$

For the aggregated protein

$$\frac{\partial C_{AJ}}{\partial t}+u\frac{\partial C_{AJ}}{\partial x}+v\frac{\partial C_{AJ}}{\partial y}=K_{D0}\exp\left[-\frac{E_D}{RT_j}\right]C^{2}_{DJ}+\frac{\partial}{\partial x}\left[D_A\left(\frac{\partial C_{NJ}}{\partial x}\right)\right]+\frac{\partial}{\partial y}\left[D_A\left(\frac{\partial C_{NJ}}{\partial y}\right)\right]-\frac{k_{mA}}{\delta_T}(C_{AJ}-C^{*}_{Ap}). \quad (14)$$

The mass balances for the various proteins in the boundary layer are as follows:

$$\frac{\partial C_{Np}^*}{\partial t} + u\frac{\partial C_{Np}^*}{\partial x} + v\frac{\partial C_{Np}^*}{\partial y} = -K_{N0}\exp\left[-\frac{E_N}{RT_j}\right]C_{Np}^* + \frac{\partial}{\partial x}\left[D_N\left(\frac{\partial C_{Np}^*}{\partial x}\right)\right] + \frac{\partial}{\partial y}\left[D_N\left(\frac{\partial C_{Np}^*}{\partial y}\right)\right] - \frac{k_{mN}}{\delta_T}(C_{Np}^* - C_{Nj}), \tag{15}$$

$$\frac{\partial C_{Dp}^*}{\partial t} + u\frac{\partial C_{Dp}^*}{\partial x} + v\frac{\partial C_{Dp}^*}{\partial y} = K_{N0}\exp\left[-\frac{E_N}{RT_j}\right]C_{Np}^* - K_{D0}\exp\left[-\frac{E_D}{RT_j}\right]C_{Dp}^{*2} + \frac{\partial}{\partial x}\left[D_D\left(\frac{\partial C_{Dp}^*}{\partial x}\right)\right] + \frac{\partial}{\partial y}\left[D_D\left(\frac{\partial C_{Dp}^*}{\partial y}\right)\right] - \frac{k_{mD}}{\delta_T}(C_{Dp}^* - C_{Dj}), \tag{16}$$

$$\frac{\partial C_{Ap}^*}{\partial t} + u\frac{\partial C_{Ap}^*}{\partial x} + v\frac{\partial C_{Ap}^*}{\partial y} = K_{D0}\exp\left[-\frac{E_D}{RT_j}\right]C_{Dp}^{*2} + \frac{\partial}{\partial x}\left[D_A\left(\frac{\partial C_{Ap}^*}{\partial x}\right)\right] + \frac{\partial}{\partial y}\left[D_A\left(\frac{\partial C_{Ap}^*}{\partial y}\right)\right] - \frac{k_{mA}}{\delta_T}(C_{Ap}^* - C_{Aj}) - k_w C_{Ap}^*, \tag{17}$$

$$\frac{\partial C_{Mp}^*}{\partial t} = \frac{k_w}{\delta_T}C_{Ap}^*. \tag{18}$$

Modeling the fouling phenomenon in the plate heat exchanger requires knowledge of several properties both at bulk and at wall conditions. Moreover, the thickness of the hydrodynamic boundary layer δ is related to that of the thermal boundary layer δ_T, by the well-known solution obtained by Eckert [7]:

$$\frac{\delta_T}{\delta} = Pr^{1/3}. \tag{19}$$

The use of the Von Karman integral theory can drive to this type of relation between δ_T and δ knowing the boundary conditions along with the velocity and temperature profiles. Furthermore, the protein mass transfer coefficient k_{mi} is related to the diffusion coefficient D_i by

$$k_{mi} = \frac{D_i}{\delta}, \tag{20}$$

where D_i can be calculated as follows [18]:

$$D_i = 1.310^{-17} \frac{T_J}{\mu V_i^{0.6}}. \tag{21}$$

The mass of protein and salt material deposited on a plate heat exchanger expressed in $\mathrm{g/m}^2$, can then be calculated as follows:

$$\mathrm{Mass}_p(x, y) = \frac{\lambda_d \mathrm{Bi}_p(x, y)\rho_d}{U_0} + tk_s \log\frac{I}{L}. \tag{22}$$

The overall heat transfer coefficient for clean conditions U_0 is calculated according to the following equation [6]:

$$\mathrm{Nu} = \frac{hD_e}{\lambda} = 0.214(\mathrm{Re}^{0.662} - 3.2)\,\mathrm{Pr}^{0.4}, \tag{23}$$

where

$$D_e = 2e_j \tag{24}$$

and

$$\frac{1}{U_0} = \frac{1}{h_c} + \frac{1}{h_f} + \frac{P_J}{\lambda_p}. \tag{25}$$

The overall heat transfer coefficient for the fouled conditions U is given by [4]:

$$U = \frac{U_0}{1 + \mathrm{Bi}}. \tag{26}$$

Biot number states on the effect of the fouling over quality of heat transfer. When the thickness of fouled deposit increases the Biot number increases also. The Biot number will change from zero (not fouling) until infinite (in theory).

The rate of deposition is related to the rate of change of heat transfer Bi_p as follows [25]:

$$\frac{\partial \mathrm{Bi}_p}{\partial t} = \beta \delta_T \frac{\partial C^*_{Mp}}{\partial t}, \tag{27}$$

where β is a constant.

The dynamic boundary layer thickness δ can be calculated from the Sherwood number Sh by the relation [5]:

$$\delta = \frac{D_e}{\mathrm{Sh}}, \tag{28}$$

where the Sherwood number is determined by

$$\mathrm{Sh} = 0.214(\mathrm{Re}^{0.662} - 3.2)\mathrm{Sc}^{0.4}. \tag{29}$$

Table 2 summarizes the methods by which physical and thermo-physical properties used in the calculations are determined. Moreover, Table 3 gives the heat exchanger data and operating conditions used in the study.

Mass depositions lead to a decrease of the hydraulic diameter during operation. This will cause the pressure drop over the structure to rise, up to the point that normal operation is not possible anymore. Clearly, pressure drop is an important parameter and will be considered as the determining factor in comparing different system layouts and process conditions.

Table 2. Evaluation of the thermo-physical properties used in the simulation [19]

Thermal conductivity of milk, $\mathrm{W/m\cdot{}^\circ C}$	$0.00133\mathrm{T} + 0.539911$
Density of milk, $\mathrm{kg/m^3}$	$1033.7 - 0.2308\mathrm{T} - 0.00246\mathrm{T}^2$
Dynamic viscosity of milk, $\mathrm{Pa\cdot s}$	$(-0.60445\mathrm{T} + 0.947)10^{-3}$
Specific heat of milk, $\mathrm{J/Kg\cdot{}^\circ C}$	$1.68\mathrm{T} + 3864.2$
Thermal conductivity of plate, $\mathrm{W/m\cdot{}^\circ C}$	16.3
Specific heat of plate, $\mathrm{J/kg\cdot{}^\circ C}$	450
Density of plate, $\mathrm{kg/m^3}$	7200
Thermal conductivity of deposit, $\mathrm{W/m\cdot{}^\circ C}$	0.5
Density of deposit, $\mathrm{kg/m^3}$	1030

Table 3. Operating conditions and technical details of the plate heat exchanger

Parameter	Symbol	Value
Flow rate, kg/s		0.074
Diameter, m	D_e	0.0022
Width of plates, m	l	0.1
Height of plates, m	l	0.1
Thickness of plates, m	P_J	8×10^{-4}
Gap between plates, m	e	4×10^{-3}
Constant	β	129
Native protein diameter, m	D_N	9.92×10^{-11}
Wall reaction rate, m/s	k_W	10^{-7}

It is considered using the classic Darcy equation for circular pipes [20], where pressure drop ΔP is determined by

$$\Delta P = \bar{f}\,\frac{\rho u^2}{2}. \tag{30}$$

The friction factor f can be calculated for turbulent flow

$$\frac{1}{\sqrt{\bar{f}}} = 4\log\left(\frac{\varepsilon}{3.7\overline{D}} + \frac{1.256}{\mathrm{Re}\sqrt{\bar{f}}}\right). \tag{31}$$

The surface roughness ε is reliant on the material of the tube. For stainless steel, a value of 0.1 mm can be supposed [18]. Some parameters for these equations are temperature or time-dependents. The temperature dependency is taken into account by using an average value for each system. The time dependency is accounted for in the same manner as for the differential equation integration. For non-isothermal flow $\bar{f}$ is not constant, and the systems under study deviate form the ideal circular pipes equation to calculate pressure drop is valid for couplings, bandings.

This necessitates the use of a correction factor [18]. Based on pressure drop measurements in system, it was found that a correction factor of 2.5 was able to reproduce the measurements within a margin of 10%. Similar measurements were not available for the other systems, but since only relative pressure drop changes are used for the optimization examples, this will not have a significant influence on the results.

3.3. Characteristics of the neural network and application

The basis element of a neural network is the neuron. It is necessary to associate to every neuron a model. The choice of this mathematical expression is fundamental. The following expression is used in the literature:

$$f(Z) = \frac{1}{1 + \exp(-\lambda_j Z)}. \tag{32}$$

Several possibilities of neurons interconnection can be defined.

In current years, the topic of adaptive neural networks has become interesting. The basic algorithm has been obtained from the Hagglund method [10], however other linear and nonlinear neural networks have been formed and improved. Architecturally, the Adaline network (Adaptive Linear Element) is identical to the Perceptron. It consists of an input layer of two neurons with feed forward connections to a single output neuron. The output node computes the linear sum *i* of the inputs *xi* from each input neuron connected to output neuron *j*, multiplied by their corresponding connection weights Γ_{ij} plus a threshold ϑ:

$$i = \sum_{i=1}^{n} \Gamma_i X_i + \vartheta. \tag{33}$$

The aim of Adaline's training algorithm is to minimize the error between the desired and achieved outputs of the network for the entire training set. The error function is given by:

$$\overline{E} = \text{Min}[f(a, \overline{b})] = \sum \frac{U}{U_0}. \tag{34}$$

The least mean square learning method obtained the values of all weights which minimize the error function $\overline{E}$ by a method called *gradient descent*. The plan is to adjust each weight by an amount proportional to the depressing of the derivative of the error when a particular input pattern is obtainable. The weight adjustment is thus set by:

$$\Delta\Gamma_{ij} = -\xi\left(\frac{d\overline{E}}{d\Gamma_{ij}}\right)^2. \tag{35}$$

The procedure used to develop and to apply the network of neurons is the following: determination of the available measures for the model and definition of

the number of entries and exits of the network, definition of a training set of vectors pairs of entries/exits, selection of a network configuration,

- Network training while using the simulation data,

- Network test by presentation of a entries set non learned and while observing the answers on the obtained exits,

- Computation of the network performance indication from the middle error enters the network exits and the simulations measures,

- If the error is acceptable, pursuit of the algorithm. Otherwise, use of another configuration and return to the third point,

- Use of the network already dragged in working according to the simulations and display of the variables of exits.

The Adaline network used in this work employed two entries, the temperature and the heat flux and the mass deposition or the global exchange coefficient as in exit.

In the process start, the heat exchanger surface is cleaned and the error is thus equal to 1. The increase of temperature milk by heating triggers the deterioration process of the proteins and sedimentation of salts, leads to the deposit that generates the fouling and the fall of the global exchange coefficient. In this situation, the error stretches toward zero and the cleaning of the heat exchanger becomes necessary.

The deposit fouling creates a new thermal resistance and causes the fall thus of thermal exchanges between the two fluids who circulate in heat exchanger (the thermal conductivity of the deposit is equal in $0.5\,W/m^{\circ}C$ [5]). It leads to a decrease of the temperature and consequently results in a bad pasteurization.

The following procedure is used to estimate the deposit mass:

- Previous results of simulation (temperature and flux) are used as reference data in order to adapt the Adaline network neuronal chosen,

- Neurones networks are introduced to indicate in evidence the operative conditions that gave a minimal error,

- Mass deposition or the overall heat transfer coefficient is calculated,

- Calculated values are compared with previous values obtained by simulation (reference).

3.4. Initial and boundary conditions

The plate heat exchanger was preceded at steady state with a non fouling fluid. This is acceptable since pasteurizers are preheated with hot water before the milk fluid is processed. The following initial conditions are then imposed and given by:

$$T_j(x,\ y,\ t) = T_0, \quad \forall j,\ \forall x,\ \forall y,\ t = 0,$$

$$T_p(x,\ y,\ t) = T_{\text{amb}}, \quad \forall p,\ \forall x,\ \forall y,\ t = 0,$$

$$C_{Nj}(x,\ y,\ t) = C_{Dj}(x,\ y,\ t) = C_{Aj}(x,\ y,\ t) = 0, \quad \forall j,\ \forall x,\ \forall y,\ t = 0,$$

$$C^*_{Np}(x,\ y,\ t) = C^*_{Dp}(x,\ y,\ t) = C^*_{Ap}(x,\ y,\ t) = 0, \quad \forall p,\ \forall x,\ \forall y,\ t = 0,$$

$$C_{Nj}(x,\ 0,\ t) = C^*_{Np}(x,\ 0,\ t) = 5\text{Kg/m}^3 \quad \forall j,\ \forall p,\ \forall t,\ x \in [0,\ 0.1],$$

$$C_{Dj}(x,\ 0,\ t) = C^*_{Dp}(x,\ 0,\ t) = 0\text{Kg/m}^3, \quad \forall j,\ \forall p,\ \forall t,\ x \in [0,\ 0.1],$$

$$C_{Aj}(x,\ 0,\ t) = C^*_{Ap}(x,\ 0,\ t) = 0\text{Kg/m}^3, \quad \forall j,\ \forall p,\ \forall t,\ x \in [0,\ 0.1]. \tag{36}$$

Top and bottom wall boundaries:

$$\frac{\partial C_{Nj}}{\partial y} = -\frac{\partial C_{Dj}}{\partial y} = \frac{\partial C_{Aj}}{\partial y} = \frac{\partial C^*_{Np}}{\partial y} = \frac{\partial C^*_{Dp}}{\partial y} = \frac{\partial C^*_{Ap}}{\partial y} = 0,\ \forall_j,\ \forall_p. \tag{37}$$

Left and right wall boundaries:

$$\frac{\partial C_{Nj}}{\partial x} = \frac{\partial C_{Dj}}{\partial x} = \frac{\partial C_{Aj}}{\partial x} = \frac{\partial C^*_{Np}}{\partial x} = \frac{\partial C^*_{Dp}}{\partial x} = \frac{\partial C^*_{Ap}}{\partial x} = 0, \quad \forall_j,\ \forall_p. \tag{38}$$

4. Results and Discussions

4.1. Numerical simulation

The model described in this paper includes a set of integral partial differential and algebraic equations. The solution method is based on a two phase method of lines approach. In the first phase, the spatial dimensions are discretized in terms of finite dimensional representations, leading to a reduction of the integral, partial differential and algebraic equations into sets of differential algebraic equations with respect to time. The second phase, the differential algebraic equations are integrated with respect to time by a modified Euler's technique [22]. Hierarchical model

construction is employed. Each channel is modeled as a sub-model. All the sub-models are eventually connected to a general model through appropriate boundary conditions. The plate heat exchanger thermal model is also defined in parallel and suitably connected with all the other sub-models to define the temperatures required by the protein reaction scheme. Different numerical methods are used for discretization, according to the flow direction. A finite difference method with 40 elements is used if the flow is in the two directions from zero to the exit of the channel. The plate heat exchanger thermal model is approximated by a second order centered finite difference method with 40 elements. This discretization schemes and orders were chosen to obtain results. Parameter estimation analysis are performed and based on the solution of a dynamic optimization problem. A regular, structured grid of plate domains in the 2D of hexahedral mesh elements was created to divide the domain into 66000 discrete elements. The domain was meshed using tetrahedral scheme.

The validation data were collected in an industrial plant with a capacity of approximately 2000 kg/h. The plant consisted of a preheating section, a heating, and cooling sections. In the following, models and the related variables are discussed. At first, the validation of the calculated values was done by comparing the deposition rates with data from the literature, then, in turn, indirectly by comparison of the simulated results with temperatures measured in an industrial heating plant. The knowledge obtained from the experiments was integrated manually into the fuzzy systems. The operating time interval considered for both simulation and validation data was set to 8h, since this was the approximate average operation time between two cleaning cycles.

4.2. Parameters of neural networks

The first step consists in defining criteria to choose the parameters of the structure according to the objectives of modeling. This criterion is defined like being the difference between the simulation value (reference) with the one obtained by the neuronal network:

$$\overline{C} = \frac{\sum_{i=1}^{n} (\overline{P}_{\text{ref}}(t_i) - \overline{P}(t_i))^2}{\sum_{i=1}^{n} \overline{P}_{\text{ref}}(t_i)^2}. \tag{39}$$

We used these criteria to study the influence of several parameters. For example, Figure 3 presents the evolution of the $\overline{C}$ criteria for the number choice of neurons in the unknown layer. One can note that the criteria of error stabilize for a number of neurons superior to 10. Beyond, the obtained results did not improve in training and in validation.

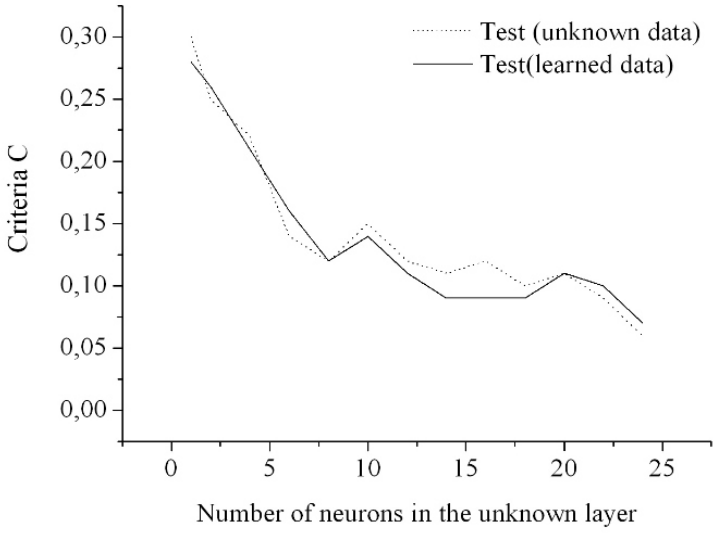

Figure 3. Criterion parameter.

The aim is to establish the fouling in the plate heat exchanger (section heating).

The fouling actions in the plate heat exchanger were investigated. The first set of data was processed using standard operation conditions (pasteurization temperature $= 90^{\circ}\mathrm{C}$) and the results are shown in Table 4. After 220 minutes of continuous operations, the unit was blocked because according to artificial neural networks, heating section had reached the minimum conditions of operation. To verify the conditions inside, the exchanger was opened and the mass deposition was established by simulation and compared with the artificial neural networks values. Table 4 illustrates that the simulation and theoretical values are very similar, indicating the good behaviour of the artificial neural networks at two-dimensional dynamic fouling simulation.

Table 4. Results in operating conditions (pasteurization temperature is $90^{\circ}C$)

Time (min)	$M_{simu}(g/m^2)$	$M(g/m^2)$
50	4.60	4.66
100	11.20	11.60
180	14.63	14.60
220	16.03	16.94

4.3. Evolution of milk temperature

The calculation of vector velocity pattern for milk in plate heat exchanger is realised by simulations performed with $\Delta x = 10\,\text{mm}$, $\Delta y = 25\,\text{mm}$, and discretized by considering $\Delta t = 0.5\,\text{s}\,(< 0.1\,\text{s})$, which satisfied the stability criterion for the explicit solution of the model. Since fluid milk flows upward through the plate surface from bottom left to top left, the model predicts a lesser amount of fluid flow on the right of plate surface, leading to an excessive temperature rise.

Figure 4 shows the milk temperature in the channel 4 of the plate heat exchanger predicted by two-dimensional dynamic fouling model after an eight (08) hours operation. The fluid enters the canal at $70^{\circ}C$ which then increases progressively the *x* and *y* two directions of the channel in an exponential fashion as the milk gains heat from the hot steam. The peaks in the temperature, recorded along the height direction are the result of thermal exchange on both sides of the considered channel. The temperature is calculated while fixing the width. At the entry of the channel adjoining plate 4, milk enters by the orifice and creates a turbulence that generates a better thermal exchange on this side in relation to the other side of the plate. This results in a more rapid progression of the temperature as opposed to the other side of the channel. Once the pasteurization temperature is reached, the thermal exchange between the two fluids is stopped.

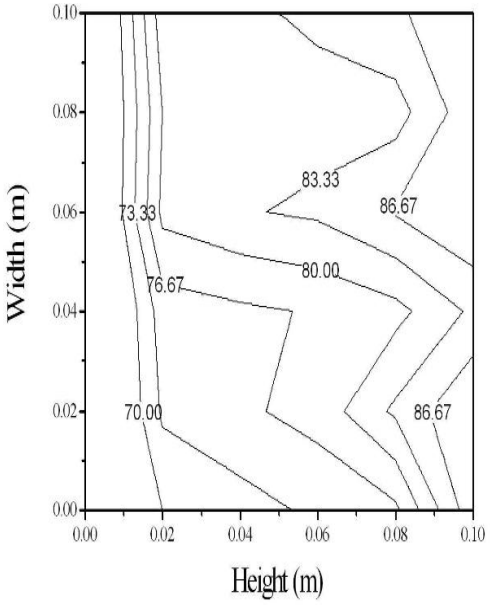

Figure 4. Simulated temperature of milk inside the 4th channel (°C).

Figure 5 shows that formation of mass deposition is directly proportional to the temperature. This result obtained by neural network indicates that the bulk and the interface temperature increase along the heat exchanger; this also increases the rate of protein and salt reactions and therefore the thickness of the layer.

These results indicate the good behaviour between the neural networks at two-dimensional dynamic fouling simulation.

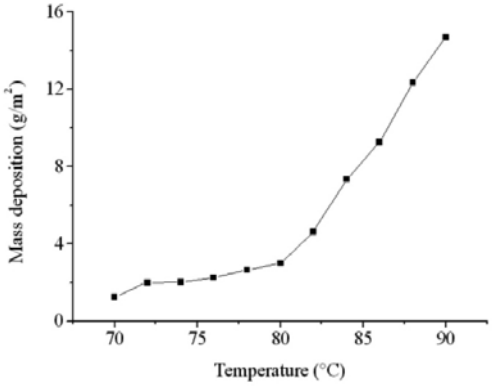

Figure 5. Effect of temperature on mass deposition.

4.4. Evolution of mass deposition

Figure 6 shows the distribution of the foulant deposition from milk in the plates of the 4th channel. The potential foulant mass per unit area is calculated to be $16\,g/m^2$ at the most. The peaks of fouling quantities, in the height direction, are due to the thermal exchanges on both sides of the considered channel (channel 4) knowing that the activation of the fouling process depends mainly on temperature. Such heat exchange becomes more important as the fluid advances in the channel. The results remain very similar to those obtained by other authors with different operating conditions but with similar type of geometry [3, 14, 17]. The deposit is primarily controlled by the protein aggregation reaction. Once heated, the proteins aggregate and stick on the wall. It is believed that the deposit of salts remains a minor phenomenon at the pasteurization temperature of $90^{\circ}C$. The faster progression of milk temperature in the entry side activates the process of fouling more quickly through the deterioration of the proteins and other saturation of salts on this side in comparison with the side opposite of the plate. This result is more important deposit of the entry of the channel of the side of the entry in relation to the contrary.

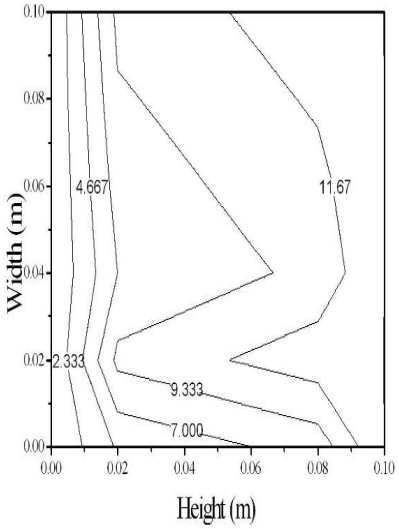

Figure 6. Fouling distribution of fluid milk in the plate adjacent to the 4th channel (g).

This result is analogous to the result found previously by neural network. The fouling phenomena increase with the temperature in the flow direction.

4.5. Evolution of the overall heat transfer coefficient

The variation of the overall heat transfer coefficient between the two fluids in the 4th channel of the heat exchanger is represented in Figure 7 obtained by two-dimensional dynamic fouling model. It is clearly established that the overall heat transfer coefficient decreases gradually along the length of the channel following the deposit formation on the plate walls which constitutes an additional layer resistant to heat exchange between the two fluids [7, 19]. Fouling growth tends to be dominant over the entire plate surface leading to a decrease of the flow rate caused by a reduction of the section crossing of flow. After a given time, the mass deposited does not affect any more the thermal exchange between the two fluids, a constant evolution of the exchange coefficient is observed. This is explained by the fact that, the value of the thickness of the deposit passes through a certain critical value after which the resistance of the fouling deposit remains appreciably constant.

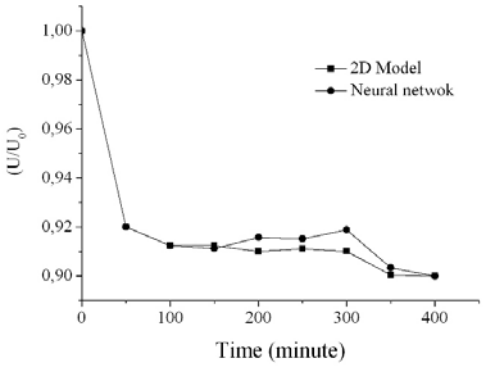

Figure 7. Evolution of the overall heat transfer coefficient.

The overall heat transfer coefficient can be observed versus time by neural network to signify the loss in process exchanger performance as the heat exchanger fouls. As expected, the overall heat transfer coefficient decreases with time is represented in Figure 7. The main reason for this type of behaviour is that the high temperatures increase the deterioration of the proteins and other saturation of salts.

These results indicate the good behaviour between the neural networks at two-dimensional dynamic fouling simulation.

4.6. Effect of Reynolds number

The mass of deposit accumulated on the plate adjacent to the 4th channel of the heat exchanger surface as a function of the Reynolds number is displayed in

Figures 8 (a, b and c) obtained by two-dimensional dynamic fouling model. Observation of these figures shows that the mass of foulant increases along the channel as mentioned. Furthermore, it also appears that the mass deposition decreases with an increase in the Reynolds number. This result is in agreement with various previous findings [2, 3] which is explained by the higher removal rate of foulant as shear forces increase. However, it should be reminded that higher Reynolds numbers values also mean higher pressure drops, which may be of considerable impaction pumping costs.

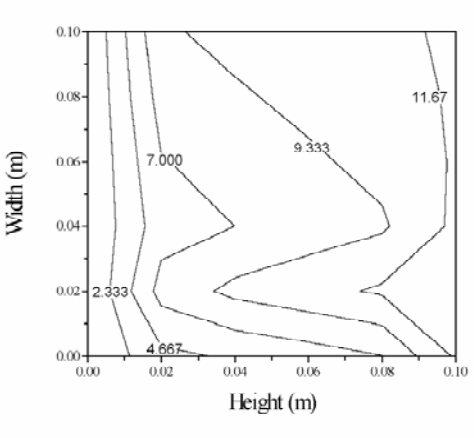

Figure 8a. Foulant mass deposition (in g) in the plate adjacent to the 4th channel for: (a) Re = 6000.

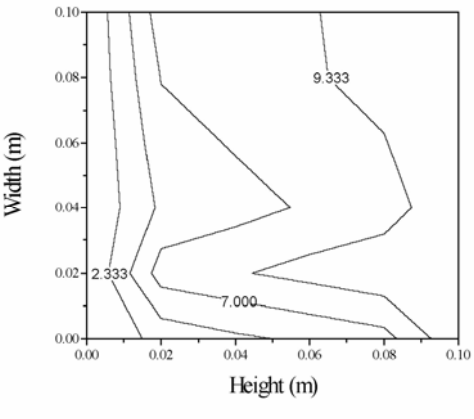

Figure 8b. Foulant mass deposition (in g) in the plate adjacent to the 4th channel for: (b) Re = 8000.

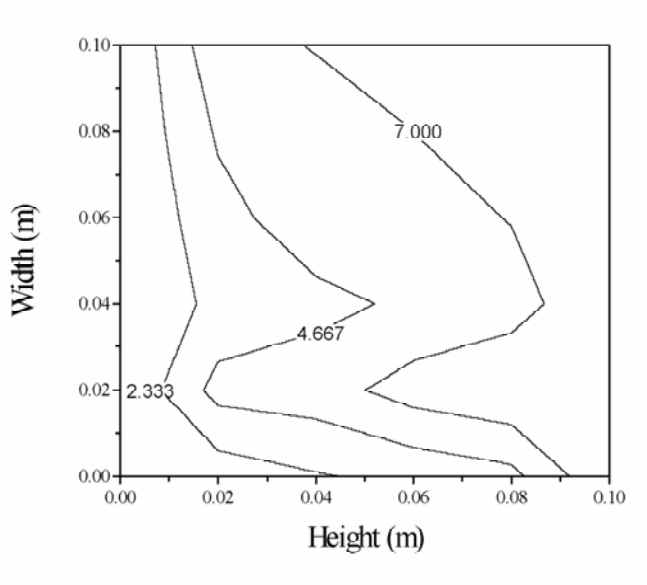

Figure 8c. Foulant mass deposition (in g) in the plate adjacent to the 4th channel for: (c) Re = 10000.

This result is in agreement with neural network simulation (Figure 9). The mass deposition decreases with an increase in the Reynolds number for the same reasons evoked previously.

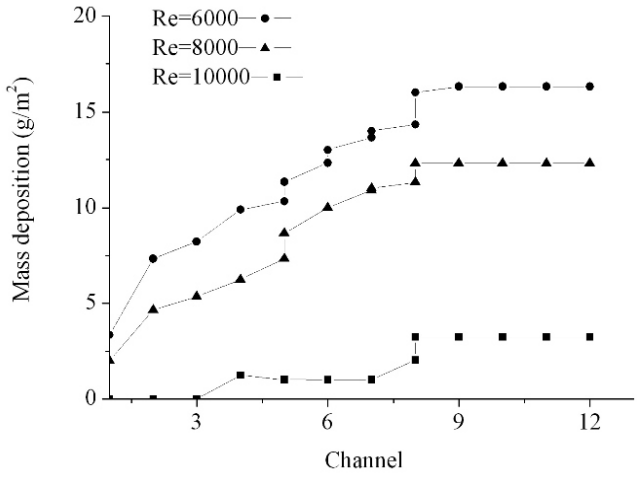

Figure 9. Effect of Reynolds number on mass deposition.

4.7. Evolution of pressure drop

The fouling forms for deposit that gives a reduction of the accessible diameter for the fluid passage, and gives pressure drop. The pressure drop is shown in Figure 10. In the same figure is represented for comparison the evolution of the pressure drop obtained with the two-dimensional dynamic fouling model. The pressure drop is the difference of pressure enters the entry and the exit of the heating section of the pasteurization system, due to the deposit on the surface of the heat exchanger. In the two situations, the pressure drop represents the formation of a deposit that increases during the working of the system due to an accumulation of the deposit on the heat exchanger surfaces of the unit. The networks of neurons counsel the stop of the working and recommended cleaning process.

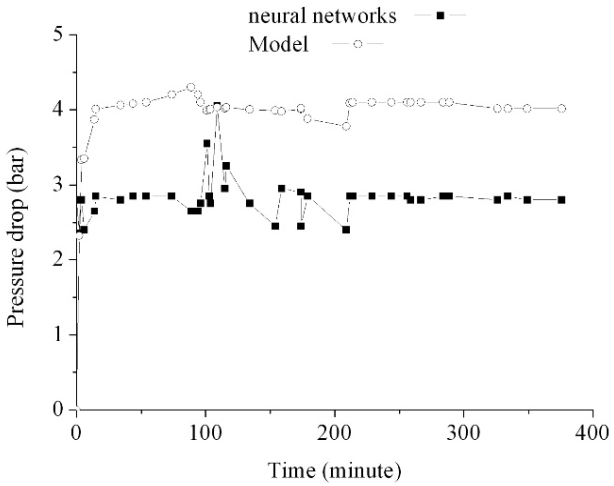

Figure 10. Evolution of the pressure drop.

These results indicate the good behaviour between the neural networks at two-dimensional dynamic fouling simulation.

5. Conclusions

A 2D fouling model, coupled with a 2D dynamic model using material balance equations for the various interactions and chemical reaction taking place during pasteurization of milk are applied to predict the performance of a plate heat exchanger subject to fouling.

The results showed fouling is highly dependent on the various process operating conditions. The different parameters seem to affect the phenomenon more specifically in the flow rather than with direction. The mass of deposit depends mainly on milk temperature and time of processing. Moreover, it is observed that the fouling extent is strongly related to the Reynolds number value and is inversely proportional to the latter.

We have developed an artificial neural networks study of plate heat exchanger under milk fouling. The networks approach permits, every time it is necessary, to put in evidence the fouling phenomena and makes thus increases the confidence in cleaning management. If the operating schedules are adequate, then it is also possible to improve the economics of the process and the quality of the milk.

For a better control of the problem, which passes by a minimization of production expenses and an optimal quality of the product, a number of solutions are recommended. For instance, a good quality of the water used is essential. Besides, a possible decrease in the pasteurization temperature is believed to allow an additional energy savings without affecting the product quality. Also, the use of food surfactants in the pasteurizer would probably contribute to create a competition during the adsorption process between the surfactant and the protein molecules which will avoid deposition on the heat exchanger surfaces. Finally, addition of an emulsifier would eventually protect the proteins from aggregating.

Acknowledgments

Dr. Mahdi would like to express his gratitude to the Professor Amrane and to Dr. Benkortbi, who contributed to the present work by their advice and the correction of the document.

References

[1] I. A. Ansari, M. Sharma and A. K. Datta, Milk fouling simulation in a double tube heat exchanger, Internat. Comput. Heat Mass Transfer 30 (2003), 707-716.

[2] M. T. Belmar-Beiny, S. M. Gotham, W. R. Paterson, P. J. Fryer and A. M. Pritchard, The effect of Reynolds number and fluid temperature in whey protein fouling, J. Food Eng. 1 (1993), 119-139.

[3] T. R. Bott and L. F. Melo, Fouling of heat exchangers, Experimental Thermal Fluid Sci. 14 (1997), 315-321.

[4] S. D. Changani, M. T. Belmar-Beiny and P. Y. Fryer, Engineering and chemical factors associated with fouling and cleaning in milk processing, Experimental Thermal Fluid Sci. 14 (1997), 392-406.

[5] P. De Jong, Modeling and optimization of thermal treatments in the dairy industry, NIZO Research Report V341 Edition, Netherlands, 1996, p. 165.

[6] F. Delaplace, J. C. Leuliet and J. P. Tissier, Fouling experiments of a plate heat exchanger by whey protein solutions, Trans. IChemE. 72(C) (1994), 163-169.

[7] E. R. G. Eckert, Introduction to the Transfer of Heat and Mass, McGraw-Hill Inc., New York, 1950.

[8] M. Georgiadis and S. Macchiatto, Dynamic modeling and simulation of plate heat exchangers under milk fouling, Chemical Eng. Sci. 55 (2000), 1605-1619.

[9] K. Grijspeerdt, L. Mortier, J. De Block and R. V. Renterghem, Applications of modeling to optimize ultra high temperature milk heat exchangers with respect to fouling, Food Control 15 (2004), 117-130.

[10] T. Hagglund, New estimation techniques for adaptative control, Ph.D. Thesis, Department of Automatic Control, Lund University, Sweden, 1983.

[11] A. S. Jeffrey and W. Nazaroff, Predicting particle deposition on HVAC heat exchangers, Atmospheric Environment 37 (2003), 5587-5596.

[12] T. J. M. Jeurnink, Fouling of milk with various calcium concentrations, Presented at Fouling and Cleaning in Food Processing, Jesus College, Cambridge, University, UK, 1994.

[13] M. Lalande and F. Reno, Fouling by milk and dairy product and cleaning of heat exchange surfaces, Fouling Science and Technology, L. F. Melo, T. R. Bott and C. A. Bernardo, eds., NATO ASI Series E, Kluwer, Amsterdam, Netherlands, 1988, pp. 557-573.

[14] M. Lalande, J. P. Tissier and G. Corrieu, Fouling of a plate exchanger used in ultra-high-temperature sterilisation of milk, J. Dairy Res. 51 (1984), 557-568.

[15] M. Lalande, J. P. Tissier and G. Corrieu, Fouling of heat transfer surfaces related to β-lactoglobulin denaturation during heat processing of milk, Biotechnology Progress 1 (1985), 131-139.

[16] S. Lalot and S. Lecoeuche, Online-fouling detection in electrical circulation heaters using neural networks, Internat. J. Heat Mass Transfer 46 (2003), 2445-2458.

[17] P. K. Nema and A. K. Datta, A computer based solution to check the drop in milk outlet temperature due to fouling in a tubular heat exchanger, J. Food Eng. 71 (2005), 141-156.

[18] R. H. Perry and D. Green, Perry's Chemical Engineering Handbook, McGraw-Hill, New York, 1984.

[19] C. Riverol and V. Napolitano, Estimation of the overall heat transfer coefficient in a tubular heat exchanger under fouling using neural networks, application in a flash pasteurizer, Internat. Commun. Heat Mass Transfer 29 (2002), 453-457.

[20] C. Riverol and V. Napolitano, Estimation of fouling in a plate heat exchanger through the application of neural networks, J. Chemical Tech. Biotech. 80 (2004), 594-600.

[21] C. Riverol and B. O'Connor, Adaptive fuzzy control as advanced control technique in milk pasteurization, FOODSIM, Blarney, Cork, 2002, pp. 454-457.

[22] P. K. Saho, I. A. Ansari and A. K. Datta, Milk fouling simulation in helical triple tube heat exchanger, J. Food Eng. 69 (2005), 235-244.

[23] G. Shetty and S. Chellam, Predicting membrane fouling during municipal drinking water Nan filtration using artificial neural networks, J. Membrane Sci. 217 (2003), 69-76.

[24] J. P. Tissier, M. Lalande and G. Corrieu, A study of milk deposit on a heat exchange surface during ultra-high-temperature treatment in engineering and food, Engineering Sciences in the Food Industry, Vol. 1, B. M. McKenna, ed., Applied Science Publishers, 1984.

[25] I. Toyoda and P. J. Fryer, A computational model for reaction and mass transfer in fouling from whey protein solutions, Fouling Mitigation of Industrial Heat Exchange Equipment, Begell House, New York, 1997.

[26] J. Visser and T. J. M. Jeurnink, Fouling of heat exchangers in the dairy industry, Exp. Thermal Fluid Sci. 14 (1997), 407-424.

[27] J. Zhang, A. Morris, E. Martin and C. Kiparissides, Estimation of impurity and fouling in batch polymerization reactors through the application of neural networks, Comput. Chem. Eng. 23 (1999), 301-314.